A ONE DIMENSIONAL HYDRAULIC MODEL FOR CONFINED NAVIGATION WITH A LONGITUDINAL VARIATION OF THE HULL

Julien Dambrine, Laboratoire de Mathématiques et Applications (UMR 7348), CNRS, University of Poitiers, France.

Valentin Jules, Institut Pprime (CNRS UPR 3346), CNRS, University of Poitiers, ISAE-ENSMA, France.

Pierre-Jean Pompée, Voies Navigables de France, France.

Morgan Pierre, Laboratoire de Mathématiques et Applications, (UMR 7348) University of Poitiers, France.

Germain Rousseaux, Institut Pprime (CNRS UPR 3346), CNRS, University of Poitiers, ISAE-ENSMA, France.

A ONE DIMENSIONAL HYDRAULIC MODEL FOR CONFINED NAVIGATION WITH A LONGITUDINAL VARIATION OF THE HULL

JULIEN DAMBRINE, LABORATOIRE DE MATHÉMATIQUES ET APPLICATIONS (UMR 7348), CNRS, UNIVERSITY OF POITIERS, FRANCE.
VALENTIN JULES, INSTITUT PPRIME (CNRS UPR 3346), CNRS, UNIVERSITY OF POITIERS, ISAE-ENSMA, FRANCE.
PIERRE-JEAN POMPÉE, VOIES NAVIGABLES DE FRANCE, FRANCE.
MORGAN PIERRE, LABORATOIRE DE MATHÉMATIQUES ET APPLICATIONS, (UMR 7348) UNIVERSITY OF POITIERS, FRANCE.
GERMAIN ROUSSEAUX, INSTITUT PPRIME (CNRS UPR 3346), CNRS, UNIVERSITY OF POITIERS, ISAE-ENSMA, FRANCE.

SUMMARY

This paper addresses some aspects of shallow water theories used for the description of the flow around boats in the context of confined navigation. We start by giving a brief account of the derivation of the most general version of the shallow water system of equations for a boat with non-constant beam and draught profiles. We will also consider the boat to be able to trim and sinkage by hydrostatic effects. Then, we present a quick review of the two classical families of theories of the literature on the matter: the energy and momentum approaches. We will comment their consistencies or inconsistencies with regards to the aforementioned general model. Finally, some numerical results are presented on the general model and comparisons with classical approaches such as the one proposed by Kreitner (1934), Schijf (1949) and Constantine (1960) will be shown.

NOMENCLATURE

CFD	Computational Fluid Dynamics
CNR	Compagnie Nationale du Rhône
KSC	Kreitner-Schijf-Constantine
t-KSC	trapezoidal Kreitner-Schijf-Constantine

An	Anthony number (Fourdrinoy et al. 2019)	
B	Boat's beam (function)	m
B_{max}	Boat's maximal beam	m
Fn_h	Froude number based on h and V	
Fn_{Hm}	Froude number based on the average depth $Hm = A_c/W$ (trapezoidal channel)	
g	Earth's gravitational acceleration (9.81m$/$s^2)	m$/$s^2
h	Canal's section maximal depth	m
I_b	Tensor of inertia of the boat	kg m^2
L_{wl}	Length of the boat (at the waterline, at rest)	m
m	Blockage ratio or Bossut number (Bossut 1775)	
m_b	Mass of the boat	kg
p	Canal's walls slope with respect to the vertical direction	
R_i	Moment of inertia ratio	
R_m	Mass ratio	
Sr	Sretensky number (Sretensky 1936)	
T	Boat's draught (function)	m
Td	Trapezoidal deviation	
T_{max}	Boat's maximal draught	m
u	Return current velocity	m$/$s
V	Horizontal speed of the boat	m$/$s
W	Canal's section maximal width	m
w	Canal's section minimal width	m
x^*	Centre of mass relative position (0 : stern ; 1 bow))	
x_b	Horizontal coordinate of the bow (w.r.t the centre of mass)	m
x_s	Horizontal coordinate of the stern (w.r.t the centre of mass)	m
z	Water level drawdown	m

$\overline{z}$	Boat's squat (from rest)	m
θ	Boat's trim (from rest)	rad
μ	Water depth to boat length ratio	
ρ	Water's mass density (1000kg$/$m^3)	kg$/$m^3

1 INTRODUCTION

The launch of major waterway expansion projects for inland water transport is currently driving the development of inland navigation, which is recognised as a mode of transport with significant economic and environmental potential (Bouman et al. 2017; Pompée 2015). However, this type of navigation has a direct impact on the balance of river ecosystems, as the waves generated by boats disturb the banks of rivers and canals.

In contrast to maritime navigation, inland navigation takes place in a confined environment in which the waterways are limited in both width and depth. These special conditions significantly influence the behaviour of boats, leading to pronounced effects such as increased squat, greater resistance to forward motion, lower propulsion efficiency, and reduced manoeuvrability.

These phenomena are inherently complex and depend on a variety of factors: the geometry of the waterway, the shape and speed of the boat, the velocity and direction of the current, and the presence of sediments and obstacles. A thorough understanding of these interactions is crucial, not only to minimise the environmental impact of inland navigation, but also to ensure safety and optimise the efficiency of navigation operations.

Several attempts have been made in the literature to describe the mechanisms governing these phenomena: vertical, lateral, and/or sectional confinement. Ranging from early studies based on fundamental physical theories proposed by Thiele (1901) or Rassmussen (Biles 1908) to more recent investigations employing advanced CFD (Computational Fluid Dynamics) techniques as in (Gourlay 2000; Bechthold and Kastens 2020; Nieutin-Redon 2024).

This paper addresses key aspects of shallow water theories applied to confined navigation. We begin by deriving the most general formulation of the shallow-water equations, which has been adapted to account for boats with non-uniform beam and draught profiles. The model also incorporates hydrostatic effects that allow for trim and sinkage (lowering of the centre of gravity) of the boat, thus extending its relevance to practical applications. In the context of the current article, we will call this model the "general model".

This is followed by a brief overview of the two classical families of theories in the literature: the energy-based and the momentum-based approaches. In most of these works, the flow is considered one-dimensional, with no head losses, and assumes a constant canal cross section that is rectangular or, more generally, trapezoidal. Similarly, the boat is modelled as a rectangular block with a constant cross section. This simplification underpins the works of Thiele (1901), Kreitner (1934), Schijf (1949), and Constantine (1960), which we will refer to as the KSC (Kreitner-Schijf-Constantine) theory throughout this article.

More recently, an analytical calculation has been provided (Pompée 2015; Delefortrie et al. 2024), ultimately offering a comprehensive summary and detailed mathematical formulations of these theories, offering valuable insights into their underlying principles and calculations. These studies used the energy-based approach, as did Marchal (1975), who extended the framework by incorporating head losses due to wall friction, as well as those occurring in wave crests, troughs, and hydraulic jumps. In addition, Marchal accounted for dynamic squat effects, providing a more comprehensive representation of real-world conditions.

In contrast, other research work, such as those of Sharp and Fenton (1968), Bouwmeester, Drost, and Van der Meer (1986) and Tenaud & CNR (Compagnie Nationale du Rhône) (1977) adopted the so-called "momentum conservation" approach. Although this method offers an alternative perspective, it is ultimately limited by the discontinuity of the flow at the bow of the vessel, which renders the momentum-based approach inconsistent with the classical shallow-water theory (and thus our model). We mention that Chen (2013) proposed a model that is very similar to the one shown here, but with additional terms (transverse flow, thickening of the boat by boundary layer effects, first-order dispersive effects), which takes into account phenomena that are far beyond the scope of the present work.

Their consistencies and limitations are critically assessed in light of the aforementioned "general model". This comparative analysis highlights the conditions under which these traditional theories align or deviate from the behaviour predicted by the general model in the limit of a block boat.

Finally, numerical simulations of the general model are performed, and the results are compared with the classical KSC theories adapted to trapezoidal section canals (Jules et al. 2024), called t-KSC (trapezoidal Kreitner-Schijf-Constantine) in the context of this article. The results provide valuable insight into the dynamics of confined navigation and suggest possible improvements to existing theoretical frameworks. Further, the results compared with classical theories illustrate the impact of this asymmetry on the boat's trim and overall hydrodynamic behaviour.

2 DERIVATION OF THE GENERAL SHALLOW-WATER MODEL

Let us consider a waterway with a constant trapezoidal section, we denote $\vec{e}_x$ the unit vector indicating the longitudinal direction (pointing forward), $\vec{e}_y$ the transverse unit vector, and $\vec{e}_z$ the upward unit vector. We denote Ω the fluid domain, Γ_f the free surface (time dependent), Γ_c the walls and bottom of the waterway, and Γ_b the boundary (time dependent) of the boat immersed in fluid. We assume that the boat is moving at a constant speed V along the $\vec{e}_x$ axis and is free to move vertically and to trim. The frame of reference is following the boat that is moving forward with constant speed V. The origin of the frame of reference is set at the intersection between the vertical axis passing through the centre of mass of the boat and the horizontal plane that coincides with the water level at rest. Let $S(x) = (]x-\varepsilon/2, x+\varepsilon/2[\times\mathbb{R}^2)\cap\Omega$ be a transverse

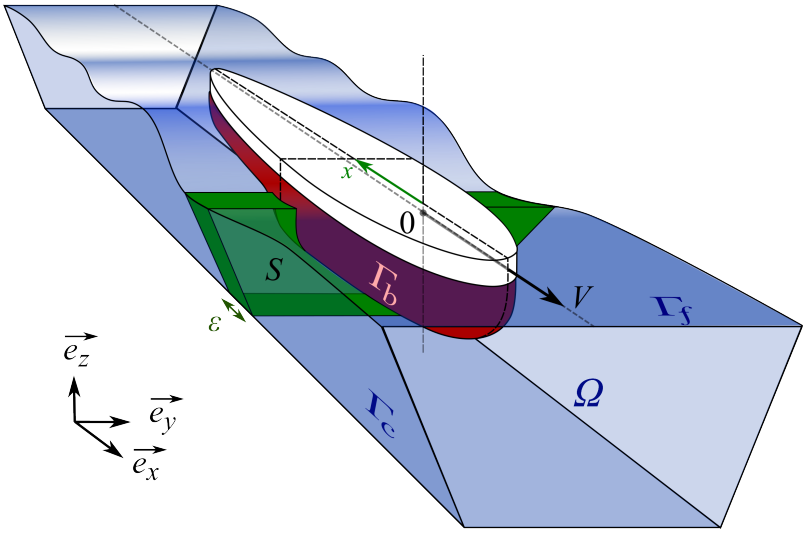

Figure 1: Geometric setting of the problem and main notations for the fluid and boat's domains.

slab of the fluid domain, centred on the longitudinal coordinate $x \in \mathbb{R}$, with thickness ε (see figure 1). Let us denote Σ_+ and Σ_- the front and back boundaries of the slab, and let us denote, respectively, Σ_c, Σ_b, Σ_s, the boundaries of S in contact, respectively, with the waterway, the boat and the free surface. The conservation of mass and momentum in S for an inviscid incompressible fluid write (Batchelor 1967):

$$\frac{d}{dt}|S| = \int_{\Sigma_\pm} \vec{U}\cdot\vec{n}\,ds, \tag{1}$$

$$\frac{d}{dt}\int_S \vec{U}d\vec{r} = -\int_{\Sigma_\pm}\left(\vec{U}\otimes\vec{U}\right)\vec{n}ds - \frac{1}{\rho}\int_S \nabla P dx - g\,|S|\,\vec{e}_z, \tag{2}$$

where $|S|$ denotes the volume of S, $\vec{U}$ is the fluid's velocity, P is the fluid's pressure, ρ is the water's mass density and g is the Earth's gravitational acceleration. In addition to these conservation equations for the fluid, we shall consider the following equations for the conservation of the linear and angular momentum of the boat (Landau and Lifshitz 1976):

$$\frac{d}{dt}\left(m_b\vec{U_b}\right) = -\int_{\Gamma_b} P\vec{n}\,\mathrm{d}s - m_b g\vec{e_z}\,, \tag{3}$$

$$\frac{d}{dt}\left(I_b\,\vec{\omega_b}\right) = -\int_{\Gamma_b} P\,\vec{r}\wedge\vec{n}\,\mathrm{d}s - m_b g\,\vec{r_g}\wedge\vec{e}_z, \tag{4}$$

where $\vec{U_b}$ is the velocity of the boat's centre of mass, m_b is the mass of the boat, $\vec{\omega_b}$ is the boat's angular speed, and I_b is its inertia tensor. Since the origin of the reference frame is placed on a vertical line that passes through the centre of gravity of the boat, we have $\vec{r_g}\wedge\vec{e}_z = 0$. The next section introduces some hypotheses about the dynamics of the boat along with some notation of its geometric parameters and kinematic variables.

2.1 BOAT'S GEOMETRY AND KINEMATICS

Recall that it is assumed that the boat moves horizontally at constant speed V. The displacement and rotation of the boat are governed by equations (3), (4). In the context of this article, we will call "sinkage" the vertical displacement of the boat and "trim" the angle of rotation of the boat along the $\vec{e_y}$ axis starting from the rest configuration. It is important to note that in the literature a distinction is made between sinkage and trim induced by hydrostatic effects (solely due to the buoyancy forces)

and sinkage and trim induced by hydrodynamic effects. In the scope of this paper, as we will see later, the only components of the sinkage and trim are the hydrostatic ones. Let $\overline{z}$ be the sinkage and let θ be the trim angle (positive for an upward displacement of the bow). We have, in the frame of reference following the horizontal motion of the boat (as described in the previous section):

$$\vec{U}_b(t) = -\dot{\overline{z}}(t)\vec{e}_z\,, \quad \vec{\omega}_b(t) = \dot{\theta}(t)\vec{e}_y\,. \tag{5}$$

The left-right symmetry of the boat implies that:

$$I_b\vec{e_y} = I_y^0 m_b\,\vec{e_y}\,, \tag{6}$$

where I_y^0 is the boat's principal moment along $\vec{e}_y$. For simplicity, we also assume that all sections of the boat are rectangular (with a beam B and a draught T).

The domain of the boat at rest is hence (see figure 2, top row):

$$\Omega_b^0 = \{\vec{r} \in \mathbb{R}^3 \;|\; |r_y| < B(r_x)/2, \text{ and } r_z > T(r_x)\}. \tag{7}$$

With a vertical displacement $\overline{z}(t)$ and trim angle $\theta(t)$ (see figure X, bottom row), it can be shown that, at first order with respect to θ the domain of the boat becomes:

$$\Omega_b^{\overline{z},\theta} = \{\vec{r} \in \mathbb{R}^3 \;|\; |r_y| < B(r_x)/2, \text{ and } r_z > T(r_x) + r_x\theta - \overline{z}\}. \tag{8}$$

The hypothesis that the trim angle is small is consistent with the "long boat hypothesis" that will be introduced in the next section. This implies that, in first order, the effect of a sinkage and trim can be seen as a modification of the draught profile of the boat. Let us also introduce the following notation:

- The surface area of the section of the waterway at rest:

  $$A_c = \frac{W+w}{2}\,h\,, \tag{9}$$

  where W (respectively w) is the canal's section maximal (respectively minimal) width, and h is the canal's section maximal depth. Since $w = W - 2ph$ (by definition of p, see figure 2), we have:

  $$A_c = \frac{W + (W-2ph)}{2}\,h = (W - ph)\,h\,. \tag{10}$$

- The surface area of the section the immersed part of the hull at longitudinal coordinate x and time t:

  $$A_b(x, z, \overline{z}, \theta) = B(x)\left(\overline{z} - x\theta + T(x) - z\right)^+\,, \tag{11}$$

  where $(\cdot)^+$ denotes the positive part, and we recall, from figure 2 that z is the free surface drop profile. Since it introduces both theoretical and numerical challenges, this threshold effect will be ignored later on as we will assume that the free surface shall never drop below the boat in reasonable situations.

- The surface area of the section of the waterway at longitudinal coordinate x and time t:

  $$A_w(x, z, \overline{z}, \theta) = A_c - A_b(x, z, \overline{z}, \theta) - z(W - pz)\,. \tag{12}$$

Let us note that in the above definitions, A_b and A_c appear to be independent of time, which is wrong in general: both A_b and A_c depend on the functions θ, $\overline{z}$, and z, which, depending on the context, can be functions of time. For example, the surface area of the boat at time t and longitudinal coordinate x is given by $A_b(x, z(t,x), \overline{z}(t), \theta(t))$.

2.2 FLOW HYPOTHESES

We now assume that the variations of the boat's geometrical parameters $T(x)$ and $B(x)$ are slow along the longitudinal coordinate, *i.e.*:

$$hT'(x)/T_{max} << 1\,, \quad hB'(x)/B_{max} << 1\,, \tag{13}$$

where T_{max} and B_{max} are respectively the maximum draught and beam of the boat. Note that, for a boat with length L_{wl}, if we suppose that the dimensionless beam and draught profiles ($T(x/L_{wl})/T_{max}$ and $T(x/L_{wl})/T_{max}$) are fixed, then assuming (13) is equivalent to suppose that:

$$h/L_{wl} << 1\,. \tag{14}$$

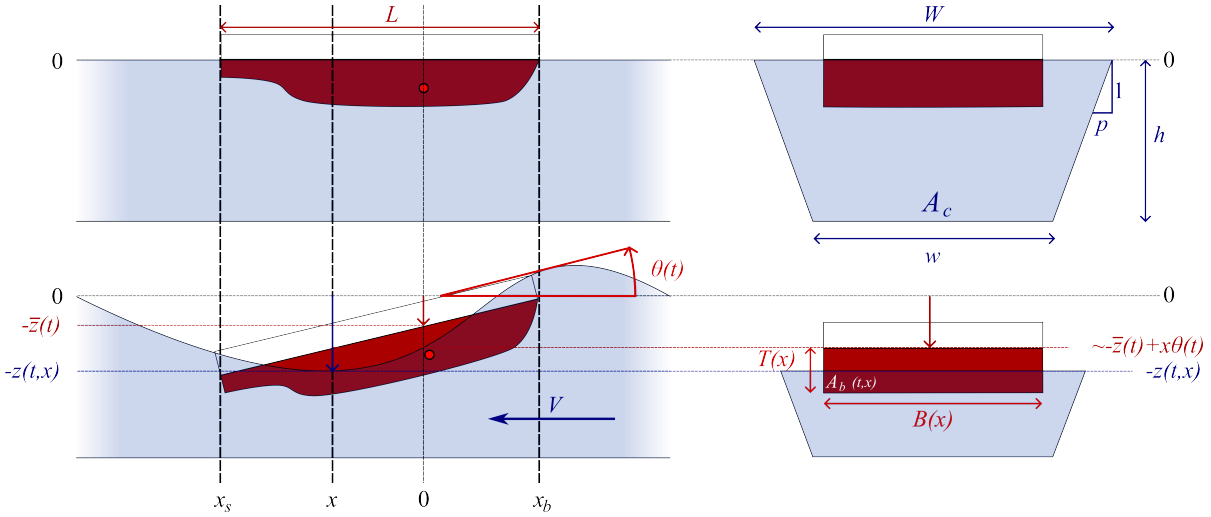

Figure 2: **Notation for the main geometrical variables involved in the model. Top row: boat at rest : bottom row: boat in motion. left column: side view, right column: front view for a slice at longitudinal coordinate x**

These assumptions, which we will refer to as the "long boat hypothesis", will lead us to assume that the flow is slowly varying along the longitudinal axis of the waterway and that the pressure can be assumed to be at hydrostatic equilibrium on every section of the canal (Saint-Venant hypotheses on the flow). We hence first assume that the flow is unidirectional and uniform across each section:

$$\vec{U}(\vec{r}) = -\left(u(r_x) + V\right)\vec{e_x}\,, \tag{15}$$

where u is the return current velocity (negative in the $\vec{e}_x$ direction). Second, the pressure is at hydrostatic equilibrium for each section:

$$P(\vec{r}) = -\rho g\left(r_z + z(r_x)\right)\,. \tag{16}$$

The first consequence of this is that no transverse variations are taken into account, and hence the free surface elevation is constant on each section:

$$\Gamma_f = \left\{(r_x, r_y,\ -z(r_x))\ ;\ r_x \in \mathbb{R}\,, r_y \in]-W/2, W/2[\right\}\,, \tag{17}$$

where z is a function that represents the water drawdown longitudinal profile. Note that this hypothesis was already implicitly introduced in the previous section (through the definitions of A_c and A_w). Since the hypotheses (13) are consistent with a flow forced by a smooth and long obstacle (albeit not necessarily thin), it is, in principle, excluded to consider boat geometries that have discontinuous variations, such as "block"-type boats. We will therefore assume that, at least, the beam profile B is continuous and that there exist two longitudinal coordinates x_s (for stern) and x_b (for bow) such that $B(x_s) = B(x_b) = 0$.

By injecting (15), (16) and (17) into the mass and momentum balance equations (1)-(2) and taking the limit $\varepsilon \to 0$ we obtain after some calculations (which will be detailed in an upcoming review paper on this topic) :

$$\underbrace{\partial_t A_w}_{\frac{1}{\varepsilon}\frac{d}{dt}|S|} + \underbrace{\partial_x\left(A_w\left(V+u\right)\right)}_{-\frac{1}{\varepsilon}\int_{\Sigma_\pm}\vec{U}\cdot\vec{n}\,ds} = 0\,, \tag{18}$$

$$\underbrace{\partial_t\left(A_w(V+u)\right)}_{-\frac{1}{\varepsilon}\frac{d}{dt}\int_S \vec{U}d\vec{r}} - \underbrace{\partial_x\left(A_w(V+u)^2\right)}_{\frac{1}{\varepsilon}\int_{\Sigma_\pm}\left(\vec{U}\otimes\vec{U}\right)\vec{n}ds} + \underbrace{gA_w\partial_x z}_{-\frac{1}{\varepsilon}\frac{1}{\rho}\int_S \nabla P dx - g|S|\vec{e}_z} = 0\,. \tag{19}$$

where the terms indicated below the following equations show the origin of the terms above in the limit $\varepsilon \to 0$. Note that in the above equation, we identified, by a small abuse of language, the function $(t,x) \mapsto A_w(x, z(t,x), \overline{z}, \theta)$ with a function of space and time A_w taken as an unknown of the system. The system (18)-(19) is a generalised version of the classical Saint-Venant system, that has been adapted to take into account the geometry of the boat implicitly through the relation between z and A_w (that we recall from 12):

$$A_w(x, z, \overline{z}, \theta) = A_c - B(x)\left(\overline{z} - x\theta + T(x) - z\right) - z(W - pz) \tag{20}$$

Let us now describe the simplified dynamics of the boat by introducing the Saint-Venant hypotheses (15), (16) and (17) in the expression of the hydrostatic forces applied to the boat's hull.

2.3 DESCRIPTION OF THE BOAT'S DYNAMICS

For $\vec{r} \in \Gamma_b$, let $\vec{F}_w(\vec{r})$ be the force exerted by the fluid on the boat at $\vec{r}$, we have:

$$\vec{F}_w = -P\,\vec{n} \tag{21}$$

Consistently with (13), since the variations of the boat's beam and draught profile are assumed to be slow with respect to the longitudinal coordinate x, we neglect the component of $\vec{F}_w$ along $\vec{e}_x$. At a given section of longitudinal coordinate x (see figure 3), we have:

$$\vec{F}_w(x, r_y, r_z) = \begin{cases} \pm\,\rho g(r_z + z(x)) & \text{on the sides } (y = \pm B(x)) \\ \rho g(-\overline{z} + x\theta - T(x) + z(x)) & \text{at the bottom } (z = \overline{z} + x\theta(t) - T(x)) \end{cases} \tag{22}$$

by symmetry, we then obtain the resultant force $\overline{\vec{F}_w}(x)$ applied at $(x, 0, -\overline{z} + x\theta - T(x))$ on the boat:

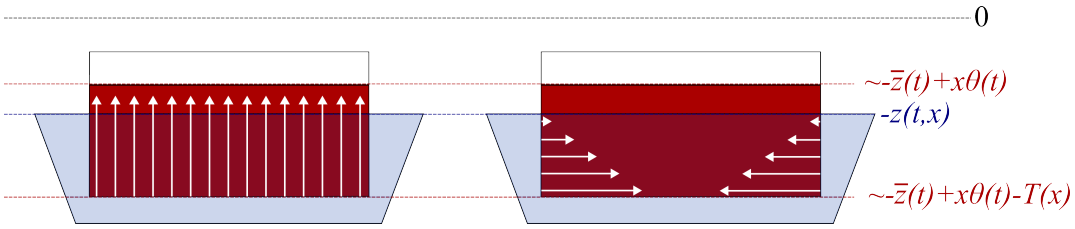

Figure 3: **Schematic description of the forces exerted by the fluid on the boat (white arrows) at a given section of longitudinal coordinate x. Left: vertical forces; right: horizontal forces.**

$$\overline{\vec{F}_w}(x) = \rho g B(x)(-\overline{z} + x\theta - T(x) + z(x))\,\vec{e}_z \tag{23}$$

Thus the total resultant force applied by the fluid on the boat writes:

$$\int_{\Gamma_b} \vec{F}_w\,\mathrm{d}s = \rho g \int_{x_s}^{x_b} \overline{\vec{F}_w}(x)\mathrm{d}x = \rho g \int_{x_s}^{x_b} B(x)(-\overline{z} + x\theta - T(x) + z(x))\mathrm{d}x\,\vec{e}_z \tag{24}$$

And the corresponding total resultant force moment writes:

$$\begin{aligned} \int_{\Gamma_b} \vec{r} \wedge \vec{F}_w\,\mathrm{d}s(\vec{r}) &= \rho g \int_{x_s}^{x_b} (x\vec{e}_x + B(x)(-\overline{z} + x\theta - T(x))\,\vec{e}_z) \wedge (-\overline{z} + x\theta - T(x) + z(x))\vec{e}_z\,\mathrm{d}x \\ &= -\rho g \int_{x_s}^{x_b} xB(x)(-\overline{z} + x\theta - T(x) + z(x))\,\mathrm{d}x\,\vec{e}_y \end{aligned} \tag{25}$$

Recalling (3)-(4) we hence have, for $(\overline{z}, \theta)$:

$$\ddot{\overline{z}}(t) = \frac{\rho g}{m_b} \int_{x_s}^{x_b} B(x)\,(\overline{z}(t) - x\theta(t) - z(t,x) - T(x))\,\mathrm{d}x + g \tag{26}$$

$$\ddot{\theta}(t) = -\frac{\rho g}{I_y^0} \int_{x_s}^{x_b} xB(x)\,(\overline{z}(t) - x\theta(t) - z(t,x) - T(x))\,\mathrm{d}x \tag{27}$$

Finally we point out the fact that at rest ($\overline{z} = 0$, $\theta = 0$, $z = 0$), the boat must be at equilibrium, hence we must have:

$$\int_{x_s}^{x_b} B(x)T(x)\,\mathrm{d}x = \frac{m_b}{\rho}\,, \quad \int_{x_s}^{x_b} xB(x)T(x)\,\mathrm{d}x = 0\,. \tag{28}$$

The first condition states that the mass of the boat must be equal to the mass of a volume of water equivalent to the immersed part of the boat at rest. It is important to note that T represents the boat's draught at rest (which will be affected, in motion, by the boat's sinkage and trim). The second condition states that, at rest, the centre of buoyancy of the boat must be at the same longitudinal coordinate as its centre of mass. Therefore, taking into account the conditions (28) in (26)-(27), we obtain:

$$\ddot{\overline{z}}(t) = \frac{\rho g}{m_b} \int_{x_s}^{x_b} B(x)\,(\overline{z}(t) - x\theta(t) - z(t,x))\,\mathrm{d}x \tag{29}$$

$$\ddot{\theta}(t) = -\frac{\rho g}{I_y^0} \int_{x_s}^{x_b} xB(x)\,(\overline{z}(t) - x\theta(t) - z(t,x))\,\mathrm{d}x \tag{30}$$

2.4 THE COMPLETE DIMENSIONLESS MODEL

In this section we rewrite our model in a dimensionless form in order to identify the key parameters of our problem. For the sake of simplicity, instead of giving a different name for the dimensionless variables, we rather rename our variables in their dimensionless form:

$$\tilde{t} = \frac{V}{L_{wl}} t\,, \quad \tilde{x} = \frac{x - x_s}{L_{wl}}\,, \quad \tilde{B}(x) = \frac{B((x-x_s)/L_{wl})}{B_{max}} \quad \tilde{T} = \frac{T((x-x_s)/L_{wl})}{T_{max}} \tag{31}$$

$$\tilde{A}_w(\tilde{t}, \tilde{x}) = \frac{A_w(\tilde{t}\, L_{wl}/V, x_s + \tilde{x}\, L_{wl})}{A_c}\,, \quad \tilde{z}(\tilde{t}, \tilde{x}) = \frac{z(\tilde{t}\, L_{wl}/V, x_s + \tilde{x}\, L_{wl})}{h}\,, \quad \tilde{u}(\tilde{t}, \tilde{x}) = \frac{u(\tilde{t}\, L_{wl}/V, x_s + \tilde{x}\, L_{wl})}{V} \tag{32}$$

$$\tilde{\overline{z}} = \frac{\overline{z}}{h}\,, \quad \tilde{\theta} = \frac{L_{wl}\theta}{h} \tag{33}$$

where $L_{wl} = x_b - x_s$, B_{max}, T_{max} represent respectively the length, maximum beam and draught of the boat (in meters). We also recall that h is the maximum upstream depth of the canal, and that:

$$A_c = h\frac{W+w}{2} = h(W - ph) \tag{34}$$

where p is the slope of the waterway with respect to the vertical direction at the border of the banks. Then, gathering the equations (18)-(19)-(29)-(30)-(12), we get the following system of dimensionless equations (again, the details will be shown in an upcoming review paper):

$$\partial_{\tilde{t}} \tilde{A}_w + \partial_{\tilde{x}}(\tilde{A}_w(1+\tilde{u})) = 0\,, \tag{35}$$

$$\partial_{\tilde{t}}(\tilde{A}_w(1+\tilde{u})) - \partial_{\tilde{x}}(\tilde{A}_w(1+\tilde{u})^2) + \frac{1}{\mathsf{Fn}_h^2}\tilde{A}_w \partial_{\tilde{x}}\tilde{z} = 0\,, \tag{36}$$

$$\tilde{A}_w(\tilde{t}, \tilde{x}) = 1 - \mathsf{Sr}\,\tilde{B}(x)(\tilde{\overline{z}}(\tilde{t}) - \tilde{z}(\tilde{t}, \tilde{x}) + \mathsf{An}\,\tilde{T}(\tilde{x}) - (\tilde{x} - x^*)\tilde{\theta}(\tilde{t}) - \frac{1}{1 - \mathsf{Td}}\tilde{z}(1 - \mathsf{Td}\,\tilde{z})\,, \tag{37}$$

$$\ddot{\tilde{\overline{z}}}(\tilde{t}) = \frac{\mu^{-2}}{\mathsf{Fn}_h^2}\mathsf{R}_m \int_0^1 \tilde{B}(\tilde{x})\left(\tilde{\overline{z}}(t) - (\tilde{x} - x^*)\tilde{\theta}(\tilde{t}) - \tilde{z}(\tilde{t}, \tilde{x})\right) \mathrm{d}\tilde{x}\,, \tag{38}$$

$$\ddot{\tilde{\theta}}(t) = \frac{\mu^{-3}}{\mathsf{Fn}_h^2}\mathsf{R}_m\mathsf{R}_i \int_0^1 (\tilde{x} - x^*)\tilde{B}(x)\left(\tilde{\overline{z}}(t) - (\tilde{x} - x^*)\tilde{\theta}(\tilde{t}) - \tilde{z}(\tilde{t}, \tilde{x})\right) \mathrm{d}\tilde{x}\,, \tag{39}$$

where, in addition to the non-dimensional beam and draught profiles B and T, the parameters of the problem are :

- Fn_h represent the maximum height-based Froude number:

  $$\mathsf{Fn}_h = \frac{V}{\sqrt{gh}}\,. \tag{40}$$

  Note that in Pompée (2015), rather than the Froude number based on h, the (cross-sectional) averaged depth based Froude number was considered:

  $$\mathsf{Fn}_{Hm} = \frac{V}{\sqrt{gH_m}} \tag{41}$$

  where $H_m = A_c/W$. This definition of the Froude number is useful in cases where p is neglected, in order to obtain an equivalent rectangular canal section for a given trapezoidal section. In our case, we retain (40) since p is taken into account in the model.

- Sr (Sretensky number) accounts for the beam to average width ratio :

  $$\mathsf{Sr} = \frac{B_{max}}{W - ph} = \frac{B_{max}}{\frac{W+w}{2}}\,, \tag{42}$$

  and An (Anthony number) accounts for the draught to depth ratio :

  $$\mathsf{An} = \frac{T_{max}}{h}\,. \tag{43}$$

  These two quantities are of crucial importance in confined hydrodynamics since they both appear in fully dispersive linear theories developed, either by Sretensky (1936) and Sretensky (1937) for the wave-making resistance in finite

depth or width, or by Keldysh and Sedov (1937) for rectangular canals. Our previous work on the battle of Actium (Fourdrinoy et al. 2019) have shown the importance of the draught to depth ratio in the outcome of this historical event, which is why we have chosen the terminology An for this ratio.

Although our model (35)-(39) is fully non-linear but non-dispersive, it is worth noticing that Sr and An also play a role here, in contrast with the KSC theory where the only geometrical ratio that matters is the blockage (or Bossut number) factor m (we recall from (10) that $A_c = (W - ph)\, h$ for a trapezoïdal canal):

$$m = \frac{B_{max} T_{max}}{(W - ph)h} = \mathsf{Sr}\,\mathsf{An} \tag{44}$$

- μ is the depth to length ratio :

$$\mu = \frac{h}{L_{wl}} \tag{45}$$

in principle this quantity is assumed to be small from (13). This suggests that the system (35)-(39) should have properties of a slow-fast system, and that a quasi-static version of (38)-(39) should be considered even in the case of a time-dependent solution of the full system. This is of little importance here as we will only seek stationary solutions.

- Td is the trapezoidal deviation :

$$\mathsf{Td} = p\frac{h}{W} = \frac{1}{2}\frac{W - w}{W} \tag{46}$$

that measures how much the section of the canal deviates from a rectangle (in which situation its value is 0).

- R_m and R_i are mass and moment of inertia ratios:

$$\mathsf{R}_m = \frac{\rho h L_{wl} B_{max}}{m_b}\,, \quad \mathsf{R}_i = \frac{h L_{wl} m_b}{I_0^y}\,. \tag{47}$$

which are of few importance here since these constant disappear for the stationary problem.

- x^* is the relative position (between 0 and 1) of the centre of mass of the boat:

$$x^* = -\frac{x_s}{L_{wl}} \tag{48}$$

In the following section, we shall drop the $\sim$ symbol over the variables in equations (35)-(39) for the sake of clarity.

3 SUB/SUPER CRITICAL FLOWS

In this section, we seek stationary solutions of (35)-(39) , which might only exist in a particular range of the above-mentioned parameters. First, the stationary version of (35) give the flow rate conservation equation:

$$A_w(1 + u) = 1\,. \tag{49}$$

Second, the stationary version of the momentum conservation equation (36) give an equation that describes the variation of the flux of fluid momentum caused by the presence of the boat:

$$-\partial_x \left(A_w(1 + u)^2\right) + \frac{1}{\mathsf{Fn}_h^2} A_w \partial_x z = 0\,. \tag{50}$$

Let us develop the first term in the above equation:

$$-A_w(1 + u)\partial_x(1 + u) - (1 + u)\partial_x(A_w(1 + u)) + \frac{1}{\mathsf{Fn}_h^2} A_w \partial_x z = 0\,. \tag{51}$$

On one hand using (49) , we remark that $\partial_x(A_w(1 + u)) = \partial_x(1) = 0$; on the other hand, assuming $A_w \neq 0$ everywhere, we have:

$$-(1 + u)\partial_x(1 + u) + \frac{1}{\mathsf{Fn}_h^2}\partial_x z = 0\,, \tag{52}$$

which leads to :

$$\partial_x \left(\frac{(1+u)^2}{2} - \frac{1}{\mathsf{Fn}_h^2} z \right) = 0 \,. \tag{53}$$

and so, integrating with respect to x, and noting that, in the absence of a current:

$$u(x), z(x) \underset{x \to +\infty}{\longrightarrow} 0 \,, \tag{54}$$

we have:

$$(1+u)^2 - \frac{2}{\mathsf{Fn}_h^2} z = 1 \,. \tag{55}$$

Finally, we recall the equations (38)-(39) in the steady state :

$$\int_0^1 \begin{pmatrix} 1 \\ x - x^* \end{pmatrix} B(x) \left(\overline{z} - (x - x^*)\theta - z(x) \right) \, \mathsf{d}x = 0 \,, \tag{56}$$

which can be recast as a linear system of unknowns $(\overline{z}, \theta)$:

$$\begin{pmatrix} 1 & -\overline{x} \\ -\overline{x} & (\sigma^2 + \overline{x}^2) \end{pmatrix} \begin{pmatrix} \overline{z} \\ \theta \end{pmatrix} = \int_0^1 \begin{pmatrix} 1 \\ x^* - x \end{pmatrix} z(x) b(x) \, \mathsf{d}x \,, \tag{57}$$

where $\overline{x}$ and σ are respectively the mean and variance associated with the normalized beam profile b:

$$b(x) = B(x) / \int_0^1 B(s) \, \mathsf{d}s \,, \tag{58}$$

$$\overline{x} = \int_0^1 (x - x^*) \, b(x) \, \mathsf{d}x \,, \tag{59}$$

$$\sigma^2 = \int_0^1 (x - x^*)^2 \, b(x) \, \mathsf{d}x - \overline{x}^2 \,. \tag{60}$$

Provided that σ is non-zero (which is true provided that the boat is not described by a singular mass), the system (57) has a unique solution that writes:

$$\overline{z} = \int_0^1 \frac{\sigma^2 + \overline{x}^2 - \overline{x} \, (x - x^*)}{\sigma^2} \, b(x) z(x) \mathsf{d}x \,, \tag{61}$$

$$\theta = \int_0^1 \frac{\overline{x} + x^* - x}{\sigma^2} \, b(x) z(x) \mathsf{d}x \,. \tag{62}$$

Our problem is therefore to solve the system of equation (49) and (55), along with the relations (61)-(62). Injecting (49) in (55) and recalling the expression (37) of A_w, our problem can be reformulated as finding z satisfying

$$\left(\frac{2}{\mathsf{Fn}_h^2} z + 1 \right) \left(1 - \mathsf{Sr} \, B(x) (\overline{z} - z + \mathsf{An} \, T - (x - x^*)\theta) - \frac{1}{1 - \mathsf{Td}} z (1 - \mathsf{Td} \, z) \right)^2 = 1 \tag{63}$$

where $\overline{z}$ and θ are given by (61) and (62). We call an "admissible solution" any continuous function $z : [0,1] \to \mathbb{R}$ satisfying equation (63), with the boundary conditions (upstream and downstream): $z(0) = z(1) = 0$. From a numerical point of view, the integrals in (61) and (62) are approached with the rectangle method, and all functions z, B, T, are uniformly discretized in the interval $[0,1]$. The solution of (63)-(61)-(62) is then sought using a quasi-Newton method implemented in python with Numpy/Scipy (Harris et al. 2020; Virtanen et al. 2020). All the results obtained in this article have been produced by a Python code available at: `https://github.com/jdambrin/MASHCON/` .

3.1 RELATIONSHIPS WITH OTHER MODELS

In this section, we stress the differences between the model presented in the previous sections and some of the models of the same family (based on a shallow water approach) that can be found in the literature. The predictions of the hydrostatic sinkage and return current are usually presented in the literature as belonging to one of the two following families of physical approaches.

- Momentum-based approaches such as those found in the works of Sharp and Fenton (1968), Bouwmeester, Drost, and Van der Meer (1986) and Tenaud & CNR (1977) in which the variation of the flux of momentum between the upstream region and the region abreast of the boat is determined by a term that is supposed to model the effect of the boat's bow on the fluid. Here, the term "momentum-based approach" is an abuse of language, since the quantity of interest is the flux of momentum (or the impulsion, when divided by ρ) rather than the momentum itself.
- Energy-based approaches such as those found in the works of Kreitner (1934), Schijf (1949), Constantine (1960) in which the conservation of the total energy (or the hydraulic head, when divided by ρg) is invoked to obtain a relation between the quantities of interest (return current and waterlevel drawdown) upstream and abreast of the boat.

It should be noted that these two approaches have been shown to produce different predictions of θ and $\overline{z}$ (Sharp and Fenton 1968). This might be counter-intuitive since a balance of momentum and a balance of energy of a mechanical system should lead to the same set of equations. The key of this paradox is that both approaches, that are based on the same Saint-Venant assumptions are equivalent (indeed (50) and (55) have been shown to be equivalent in the previous section) only when B is continuous, which is not the case in all the references mentioned above in this section, in which the boat is assumed to be a block, *i.e.*:

$$B(x) = \begin{cases} 1 & \text{if } x \in [0,1] \\ 0 & \text{if } x \notin [0,1] \end{cases} . \tag{64}$$

The approach of the present paper is to suppose beforehand that B is continuous and supported in $[0,1]$, and to eventually investigate the limit where B degenerates towards (64).

We remark that by setting $B \equiv 1, T \equiv 1$, then z is constant (and equal to $\overline{z}$), $\theta = 0$, and then equation (63) becomes:

$$\left(\frac{2}{\mathsf{Fn}_h^2} z + 1\right) \left(1 - m - \frac{1}{1-\mathsf{Td}} z(1-\mathsf{Td}\, z)\right)^2 = 1 \,, \tag{65}$$

where $m = \mathsf{SrAn}$ is the obstruction parameter. We will call this equation the "t-KSC equation" (for trapezoidal Kreitner-Schijf-Constantine), that has been studied revently by Jules et al. (2024). Moreover, for a rectangular channel ($p = 0$) we retrieve the usual equation of the classical KSC theory:

$$\left(\frac{2}{\mathsf{Fn}_h^2} z + 1\right) (1 - m - z)^2 = 1 \,. \tag{66}$$

In (63), (65) and (66) it is expected that, for given values Sr, An, Td, there exist two critical values of the Froude number Fn_h^- and Fn_h^+ which are such that, only for $\mathsf{Fn}_h \in [\mathsf{Fn}_h^-, \mathsf{Fn}_h^+]$ the equation does not have a solution. For $\mathsf{Fn}_h < \mathsf{Fn}_h^-$, the flow is called subcritical ; for $\mathsf{Fn}_h > \mathsf{Fn}_h^+$, the flow is called supercritical. For the KSC equation (66) the critical Froude values can be determined analytically as calculated by Pompée (2015) and ultimately proven completely by Delefortrie et al. (2024):

$$\mathsf{Fn}_h^- = \left(2 \sin\left(\frac{\arcsin(1-m)}{3}\right)\right)^{3/2} \tag{67}$$

$$\mathsf{Fn}_h^+ = \left(2 \sin\left(\frac{\pi - \arcsin(1-m)}{3}\right)\right)^{3/2} \tag{68}$$

For the other models (63) and (65) these critical values will be estimated numerically with a search by dichotomy.

4 NUMERICAL EXPERIMENTS

In this section we present some numerical tests with a range of parameters that are chosen to be close to realistic situations, and we aim to show the effect of the boat's end profiles and the influence of the asymmetry on the main characteristics of the flow around the boat (sinkage, trim, free-surface elevation). All the tests presented here have been produced using a script developed by the authors of the present article, and available at: `https://github.com/jdambrin/MASHCON/`.

4.1 PARAMETERS

Let us consider the following set of parameters for the boat:

$$L_{wl} = 100\mathsf{m}\,, \quad B_{max} = 11.4\mathsf{m}\,, \quad T_{max} = 2.5\mathsf{m} \tag{69}$$

Which corresponds to a large Rhine class boat as defined by the European Conference of Ministers of Transport (ECMT) (1992). We will also consider two different waterways, as in Pompée (2015). However, unlike Pompée (2015), we deliberately use the same single vessel CEMT class Vb in both class IV and Vb cross sections to simplify our comparisons:

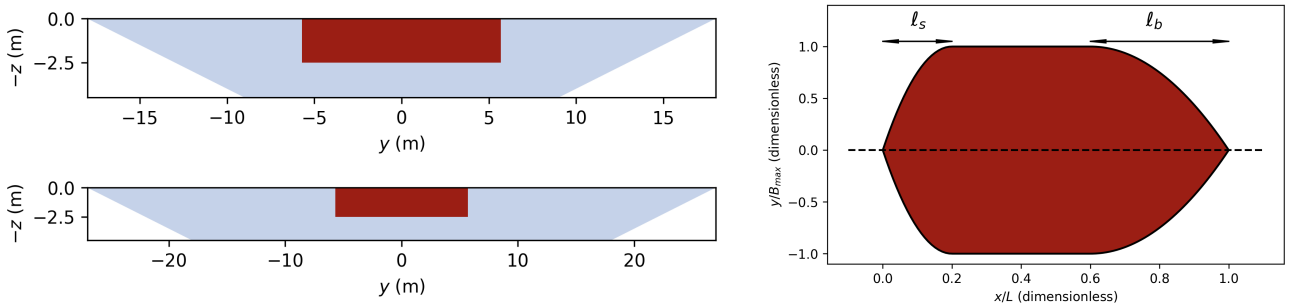

Figure 4: **Left: cross section of the canal with the boat at rest for the CEMT class IV (top) and Vb (bottom) canals; right: schematic view of the boat's beam profile, with the geometrical parameters ℓ_s and ℓ_b.**

- CEMT class IV

$$W = 36\text{m}\,, \quad p = 2\,, \quad h = 4.5\text{m} \tag{70}$$

- CEMT class Vb

$$W = 54\text{m}\,, \quad p = 2\,, \quad h = 4.5\text{m} \tag{71}$$

The figure 4 shows the cross section of the waterway and the boat at rest at the midpoint of the boat (maximum beam and draught); it shows that the main difference lies in the blockage factor (or Bossut number according to our terminology) $m = (B_{max}T_{max})/((W - ph)h)$ (which is 23% for the class IV canal and 14% for the class Vb canal). For simplicity, we will consider $T \equiv 1$ (constant draught profile), but more general profiles can be considered without any technical difficulty. The longitudinal change of the boat's section will be induced by the beam profile (prismatic boat):

$$B(x/L_{wl}) = \begin{cases} -(x/(L_{wl}\ell_s) - 1)^2 + 1 & \text{if } x/L_{wl} \in [0, \ell_s] \\ 1 & \text{if } x/L_{wl} \in [\ell_s, 1 - \ell_b] \\ -((x/L_{wl} - 1)/\ell_b + 1)^2 + 1 & \text{if } x/L_{wl} \in [1 - \ell_b, 1] \end{cases} \tag{72}$$

where ℓ_s and ℓ_b are two dimensionless parameters representing the ratio between the length of the smooth transition between the stern (respectively the bow) of the boat and the position beyond which the beam can be considered constant (see figure 4). These parameters can be related with the boat's block coefficient:

$$C_B = \int_0^1 B(s)\,\mathrm{d}s = 1 - \frac{(\ell_s + \ell_b)}{3} \tag{73}$$

and so it is clear that, as $\ell_s, \ell_b \to 0$, we have $C_b \to 1$. In this "block limit", the shape of the boat converges towards a "shoe's box" shape. The contrast between ℓ_s and ℓ_b can be related to the asymmetry of the boat :

$$a = 1 - 2x^* = -1 + 2\int_0^1 xB(x)\mathrm{d}x \Big/ \int_0^1 B(x)\mathrm{d}x\,. \tag{74}$$

A positive (r.p. negative) value of a means that the centre of gravity of the boat is towards the bow (r.p. the stern), and its maximum value is 1 (r.p. -1).

In the next sections, we will study the effect of these two geometrical parameters on the behaviour of the boat for different speeds (or Froude numbers) in the subcritical and supercritical regimes. Note that we are fully aware that such boats are never in the supercritical regime due to their incapacity to overcome the wall of resistance that appears at the end of the subcritical regime. The results in the supercritical regime are shown for theoretical interest only.

4.2 INFLUENCE OF THE END PROFILES OF THE BOAT

In this section we set $\ell_s = \ell_b = \ell$, and we investigate the behaviour of the boat as $\ell \to 0$. By symmetry arguments, it can be shown that in this particular situation we expect the trim θ to vanish. For the aforementioned values of the parameters (both class IV and Vb canals), we will compare the sinkage $\overline{z}$ as a function of the Froude number for values of ℓ ranging from 0.05 to 0.4 (which corresponds to block coefficients ranging from 0.96 to 0.73). These profiles will also be compared with the results

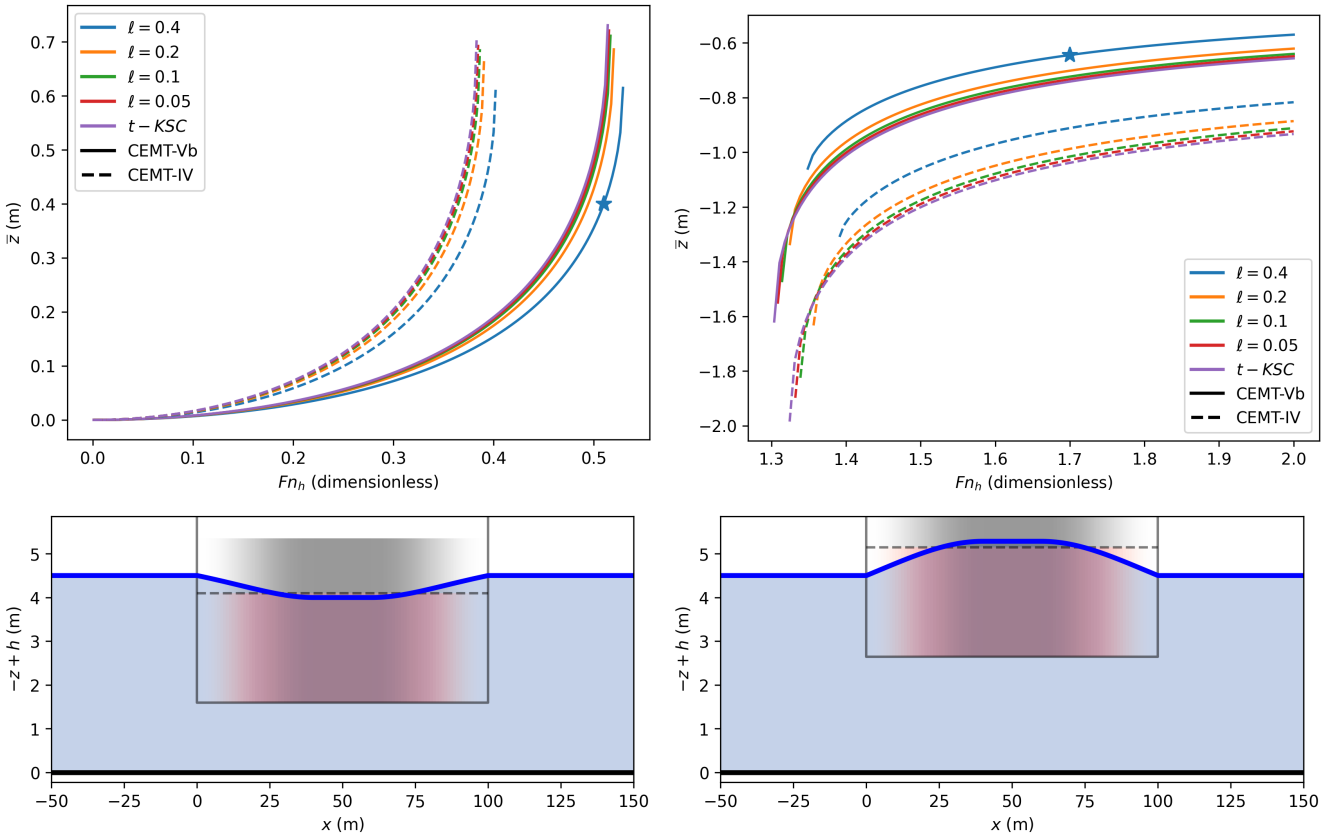

Figure 5: **Top : boat sinkage $\overline{z}$ as a function of the Froude number for the class Vb (plain) and IV (dashed) canal, and different values of the geometrical parameter ℓ. Left : sub-critical solutions ; right : supercritical solutions. Bottom : instances of the longitudinal profile of the free-surface elevation, and position of the boat (shades of red indicate the beam values), for parameters indicated by a star on the figure above.**

of the t-KSC theory (block limit). In figure 5 (top row) we can remark that, as ℓ becomes smaller, the sinkage of the boat $\overline{z}$ becomes closer and closer to the prediction of z given by the t-KSC model (purple lines), showing that the energy approach for the prediction of the hydrostatic sinkage is consistent with the Saint-Venant theory in the block limit. The tendency shown is that larger values of ℓ will give slightly larger values of the critical Froude numbers Fn_h^- and Fn_h^+ (defined in the previous section), along with a smaller maximum sinkage in the subcritical regime. The effect of larger values of ℓ therefore seems to be similar (in a nontrivial way) to smaller values of the blockage factor. For the supercritical case, the effect is inverse, as larger values of ℓ are associated with higher values of the elevation of the boat. The figure 5 (bottom row) shows instances of the longitudinal profiles of the free surface along with the boat's position for the parameters indicated by a star on the top row. These figures show that the trim is indeed null in this symmetric case.

4.3 INFLUENCE OF THE ASYMMETRY OF THE BOAT

Here, we will choose different values for ℓ_s and ℓ_b, ranging from $\ell_s = 0.4$ and $\ell_b = 0.05$ to $\ell_s = 0.05$ and $\ell_b = 0.4$ (asymmetry coefficient a ranging between -10% and 10%). The figure 6 (top) shows the trim angle as a function of the Froude number for subcritical flows (left) and supercritical flows (right). We can notice that the trim angle grows sharply in magnitude as the Froude number approaches Fn_h^-, and changes sign in the supercritical regime (where the angle seems to be changing more slowly with respect to the Froude number). One important fact to be noted here is that the sign of the angle depends on the direction of the asymmetry of the boat: if the centre of gravity is closer to the stern, the trim is bow up in the subcritical regime, and conversely, if the centre of gravity of the boat is closer to the bow, the trim is bow down in the subcritical regime.

5 CONCLUSIONS

In this article, we derived from general principles a one-dimensional hydraulic model for the flow around a boat in the context of inland navigation, that allows for regular shape profiles of the boat's beam and draught. The first feature of this model, in contrast with the more classical KSC theory, is that it requires a distinction between the water drawdown and the boat's

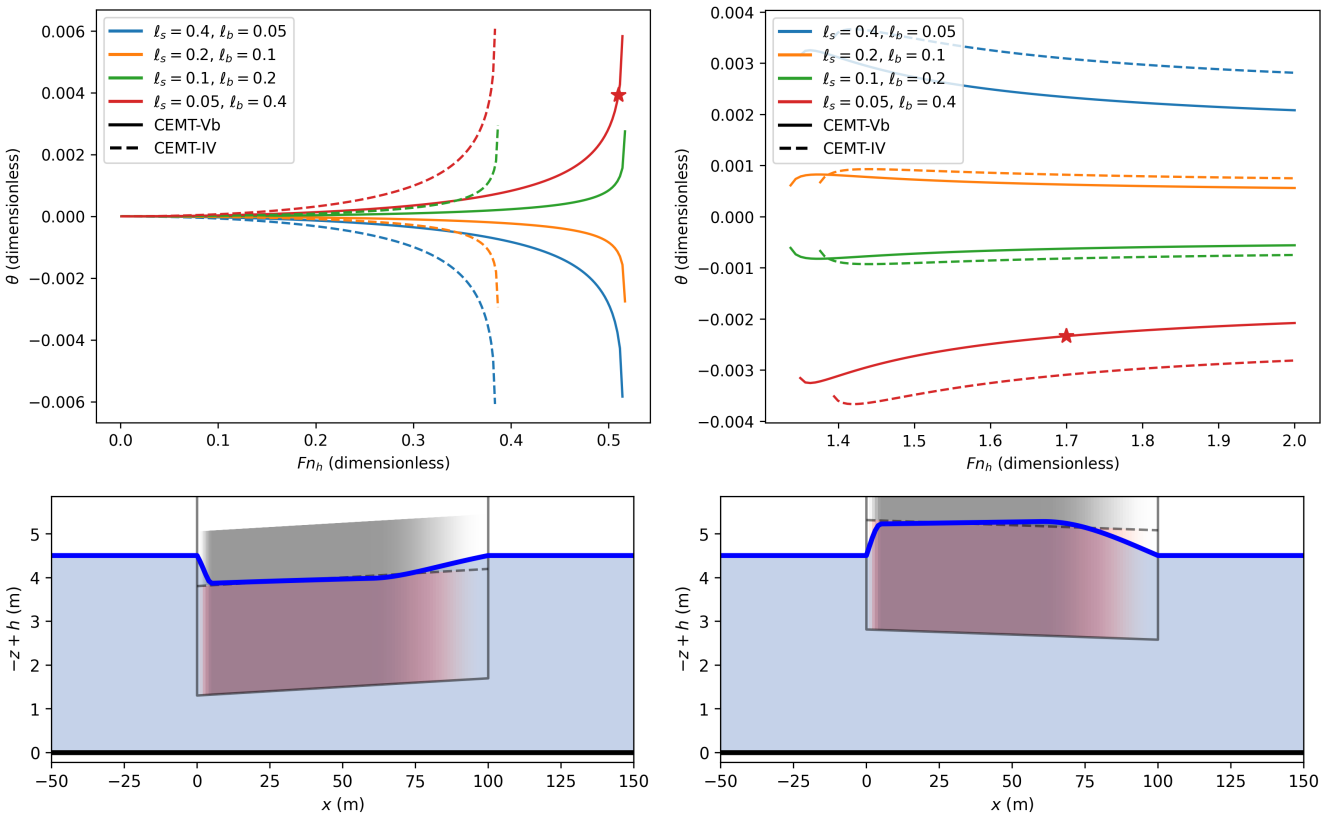

Figure 6: **Boat trim θ as a function of the Froude number for the class Vb (plain) and IV (dashed) canal, and different values of the geometrical parameters ℓ_s and ℓ_b. Left : sub-critical solutions ; right : supercritical solutions. Bottom : instances of the longitudinal profile of the free-surface elevation, and position of the boat (shades of red indicate the beam values), for parameters indicated by a star on the figure above.**

vertical displacement. The second consequence of allowing non-block boats is the emergence of a trim, merely by hydrostatic effects, induced by the longitudinal asymmetry.

Our numerical simulations, restricted to subcritical and supercritical flows, have shown that, first, when the boat's profile degenerates towards a block boat, our results converge towards the classical KSC theory adapted for canals with trapezoidal sections (t-KSC). This fact can be demonstrated formally on the systems of equations being solved, but it ought to be proven rigorously by a convergence theorem (this is a work in progress that will be the occasion of a future, more mathematical paper). Second, is the existence of the hydrostatic trim effect, which sign depends on the position of the boat's center of gravity and which is maximal in amplitude at the subcritical critical value of the Froude number Fn_h^-. We have shown that, when the centre of gravity of the boat is closer to the bow (r.p. the stern), the trim is nose-down (r.p. nose-up) in the subcritical regime and that the effect is reversed in the supercritical regime. In this study, we have always considered the draught to be constant at rest and the asymmetry being induced by variations of the beam, but it is very easy to consider, with the same model, a longitudinal variation of the draught at rest (caused, for example, by an uneven loading of the boat).

The trans-critical regime $\mathrm{Fn}_h^- < \mathrm{Fn}_h < \mathrm{Fn}_h^+$ has not been investigated here. In fact, stationary solutions to this problem do not exist in this particular situation (there is no continuous profile z of a constant specific head along the canal). This problem is usually resolved by the appearance of several hydraulic jumps: one in front of the bow (in a forward relative motion), one behind the stern (in a backward relative motion), and one abreast (stationary). Then, in the absence of friction, there is a lack of uniqueness of the position of the later stationary hydraulic jump. This suggests a position that is history dependent and justifies a future work, focused on numerical simulations of (35)-(39) which will require the design of well-balanced schemes to capture correctly the dynamics of this hyperbolic system.

These purely hydraulic models are only valid in situations of significant blockages ($m \sim 1$) and for very long vessels ($h/L_{wl} << 1$). In particular, frictional head losses, which play a role not only in the dynamics of the fluid around the vessel but also in the dynamics of the vessel itself, have been neglected here. We aim to include these effects in a future study. Finally, shallow-water theory also neglects the dispersive effects of surface waves, which are also significant in the forces exerted by the fluid on the vessel (wave resistance, lift). Accounting for precise hydraulic effects alongside dispersive effects within a framework consistent with the Euler equations poses a major challenge, which we intend to address in future work.

6 ACKNOWLEDGEMENTS

This work is funded by the French Waterways Voies Navigables de France (VNF). This work pertains (namely, is not funded but enters in the scientific perimeter) to the French government programme "Investissement d'Avenir" EUR INTREE (reference ANR-18-EURE-0010) and LABEX INTERACTIFS (reference ANR-11-LABX-0017-01).

7 REFERENCES

Batchelor, G. K., 1967. An Introduction to Fluid Dynamics. Cambridge University Press. DOI: 10.1017/CBO9780511800955.

Bechthold, Jonas and Marko Kastens, 2020. Robustness and quality of squat predictions in extreme shallow water conditions based on RANS-calculations. In: Ocean Engineering 197, p. 106780.

Biles, John Harvard, 1908. The Design and Construction of Ships (1908). Vol. 2. BoD–Books on Demand.

Bossut, Charles, 1775. Traité élémentaire d'hydrodynamique. Vol. 2.

Bouman, Evert A, Elizabeth Lindstad, Agathe I Rialland, and Anders H Strømman, 2017. State-of-the-art technologies, measures, and potential for reducing GHG emissions from shipping–A review. In: Transportation Research Part D: Transport and Environment 52, pp. 408–421.

Bouwmeester, J, JC Drost, and MT Van der Meer, 1986. Scheepssnelheiden op beperkt water met gegeven motorvermogen. Tech. rep. TH Delft.

Chen, Xue-Nong, 2013. Study of one-dimensional ship squat theories. In: Chinese Journal of Hydrodynamics 28.4.

Constantine, T, 1960. On the movement of ships in restricted waterways. In: Journal of Fluid Mechanics 9.2, pp. 247–256.

Delefortrie, Guillaume, Jeroen Verwilligen, Marc Vantorre, Evert Lataire, and Flanders Hydraulics, 2024. Exact and Approximated Solutions to the Critical Ship Speeds in Canals. In: Proceedings of the 35th PIANC World Congress.

European Conference of Ministers of Transport (ECMT), 1992. Resolution No. 92/2 on New Classification of Inland Waterways.

Fourdrinoy, Johan, Clément Caplier, Yann Devaux, Germain Rousseaux, Areti Gianni, Ierotheos Zacharias, Isabelle Jouteur, Paul-Marius Martin, Julien Dambrine, Madalina Petcu, and Morgan Pierre, 2019. The naval battle of Actium and the myth of the ship-holder: the effect of bathymetry. In: 5th MASHCON - International Conference on Ship Manoeuvring in Shallow and Confined Water with non-exclusive focus on manoeuvring in waves, wind and current, Flanders Hydraulics Research; Maritime Technology Division, Ghent University, May 2019, Ostend, Belgium. WWC007 (pp 104 - 133).

Gourlay, Tim Peter, 2000. Mathematical and computational techniques for predicting the squat of ships. PhD thesis.

Harris, Charles R., K. Jarrod Millman, Stéfan J. van der Walt, Ralf Gommers, Pauli Virtanen, David Cournapeau, Eric Wieser, Julian Taylor, Sebastian Berg, Nathaniel J. Smith, Robert Kern, Matti Picus, Stephan Hoyer, Marten H. van Kerkwijk, Matthew Brett, Allan Haldane, Jaime Fernández del Río, Mark Wiebe, Pearu Peterson, Pierre Gérard-Marchant, Kevin Sheppard, Tyler Reddy, Warren Weckesser, Hameer Abbasi, Christoph Gohlke, and Travis E. Oliphant, Sept. 2020. Array programming with NumPy. In: Nature 585.7825, pp. 357–362. DOI: 10.1038/s41586-020-2649-2.

Jules, Valentin, Pierre-Jean Pompée, Julien Dambrine, Morgan Pierre, and Germain Rousseaux, 2024. A revisit of confined medium navigation theories. In: 19e Journées de l'Hydrodynamique, Nantes.

Keldysh, M. and L. Sedov, 1937. The theory of wave drag in a channel of finite depth. In: Journal of Applied Mathematics and Mechanics 75. In "The papers of M.V. Keldysh in the field of mechanics and applied mathematics (On the centenary of his birth)", pp. 123–131.

Kreitner, J, 1934. Über den Schiffswiderstand auf beschränktem Wasser. In: Werft, Reederei, Hafen 15.7, pp. 77–82.

Landau, L. D. and E. M. Lifshitz, Jan. 1976. Mechanics, Third Edition: Volume 1 (Course of Theoretical Physics). 3rd ed. Butterworth-Heinemann.

Marchal, Jean, 1975. Contributions théorique et expérimentale au calcul de la résistance à l'avancement des convois poussés en navigation dans les voies d'eau de sections limitées. In: Collection des Publications de la FSA de l'ULg 55.

Nieutin-Redon, Pablo, 2024. Étude expérimentale et numérique des phénomènes hydrodynamiques liés au passage d'un navire dans une voie navigable confinée : quantification des ondes de batillage et de leur impact sur les berges. PhD thesis. Université de Poitiers.

Pompée, Pierre-Jean, 2015. About modelling inland vessels resistance and propulsion and interaction vessel-waterway key parameters driving restricted/shallow water effects. In: Proceedings of Smart Rivers 2015, Buenos Aires, Argentina, paper 180, September 2015.

Schijf, J.B., 1949. Protection of embankments and bed in inland and maritime waters, and in overflows or weirs. In: Proceedings of the 17th International Navigation Congress, Lisbon. SI - C2. Permanent International Association of Navigation Congresses. PIANC.

Sharp, BB and JD Fenton, 1968. A model investigation of squat. In: DOCK & HARBOUR AUTHORITY 49.577, p. 242.

Sretensky, L.N., 1936. On the wave-making resistance of a ship moving along in a canal. In: Phil. Mag. Pp. 1005–1013.

– 1937. Theoretical investigation of wave resistance. In: Transactions of the TsAGI (Central Aerohydrodynamic Institute) 319.

Tenaud & CNR, Renaud, 1977. Essais sur modèles réduits et modèles mathématiques pour l'étude du passage des convoi poussés dans un canal et des défenses des berges. In: 24th AIPCN.

Thiele, A, 1901. Schiffswiderstand auf canalen. In: Centralblatt der Bauverwaltung.

Virtanen, Pauli, Ralf Gommers, Travis E. Oliphant, Matt Haberland, Tyler Reddy, David Cournapeau, Evgeni Burovski, Pearu Peterson, Warren Weckesser, Jonathan Bright, Stéfan J. van der Walt, Matthew Brett, Joshua Wilson, K. Jarrod Millman, Nikolay Mayorov, Andrew R. J. Nelson, Eric Jones, Robert Kern, Eric Larson, C J Carey, İlhan Polat, Yu Feng, Eric W. Moore, Jake VanderPlas, Denis Laxalde, Josef Perktold, Robert Cimrman, Ian Henriksen, E. A. Quintero, Charles R. Harris, Anne M. Archibald, Antônio H. Ribeiro, Fabian Pedregosa, Paul van Mulbregt, and SciPy 1.0 Contributors, 2020. SciPy 1.0: Fundamental Algorithms for Scientific Computing in Python. In: Nature Methods 17, pp. 261–272. DOI: 10.1038/s41592-019-0686-2.

8 AUTHORS BIOGRAPHY

Julien Dambrine is assistant professor at the University of Poitiers and a member of the Laboratoire de Mathématiques et Application, as an applied mathematician working on theoretical and numerical problems involving partial differential equations for fluid dynamics. Over time he became a specialist in the mathematical modeling of wave/ship interactions in naval and, more recently, fluvial hydrodynamics.

Valentin Jules is a postdoctoral researcher at the CNRS (French National Scientific Research Center). His work focuses on theoretical modeling of navigation in confined environments.

Pierre-Jean Pompée is the responsible for Innovation Engineering at VNF (Voies Navigables de France). He is an expert in the engineering of waterways and hydraulic problems in inland navigation.

Morgan Pierre is an Associate Professor at the University of Poitiers (France). He is the head of the team "Partial Differential Equations and Applications" at the Department of Mathematics.

Germain Rousseaux is a research director at the CNRS (French National Scientific Research Center). With his team, he explained the reason for the defeat of Marc-Anthony and Cleopatra against Octavian at the naval battle of Actium because of the difference in boat draughts between both fleets and the resulting peak of wave resistance with a dedicated free surface wake. He is now interested in navigation in confined media and the effect of the return current and the water level drawdown. He is also an expert in Analogue Gravity where waterfalls mimic black holes in the laboratory.